

# LOCAL MODELS FOR NCF COMPOSITE MATERIALS MECHANICAL PERFORMANCE PREDICTION

Leif E. Asp  
SICOMP AB

**Keywords:** *NCF, CFRP, mechanical properties, RVE, RUC*

## Abstract

This paper presents models for NCF reinforced composite materials performance prediction developed within the European research project FALCOM. The research project was conducted during the years 2002 and 2005 and was led by QinetiQ, UK. In total nine European countries were represented in FALCOM.

The models consider material heterogeneity on three scales. On the micro-scale homogenization of the fibre bundle is performed. On the meso-scale formulations of Representative Volume Elements with different degrees of sophistication are defined. Finally on the macro-scale models span from straightforward employment of laminate theory to full through-thickness 3D-representation of the meso-scale features. The paper illustrates the diversity of local performance models for NCF composite analysis presenting a selection of models developed in the FALCOM project.

## 1 Introduction

Liquid-resin-infused non-crimp fabric (NCF) reinforced composites offer lower cost and improved through-thickness properties with no significant drop in in-plane performance compared to traditional tape-based composites. As such, NCFs offer new challenging possibilities to designers and manufacturers, given their higher degree of tailorability, greater deposition rate and improved impact performance when compared to their prepreg-based counterpart.

A European research project FALCOM "Failure, performance and processing prediction for enhanced design with non-crimp-fabric composites" [1] was set out with the outstanding ambition to explore, quantify and model the effects of the NCF manufacturing parameters (i.e. stitch yarn material and stitch tension, fibre tow size, inter-tow gap, etc.)

on the composite process ability and mechanical performance.

As responsible for the local modelling work co-ordination within FALCOM, the author sets out to present a summary of this work to a wider audience. Consequently, this paper presents an overview of the local material performance models development and validation within FALCOM. The presented models range from detailed Representative Volume Element (RVE) finite element models and engineering type analytical models to semi-empirical models.

## 2 Local performance models developed in FALCOM



Fig. 1. Typical NCF composite microstructure,  $[0/90/45/-45]_{S_2}$ .

The architecture of the NCFs implies that these materials are heterogeneous not only on the micro-scale but also on the meso-scale (fibre tow layers) and macro-scale (laminate). For the purpose of performance prediction, models taking the heterogeneous characteristics of NCFs on the micro- and meso-scale as well as on the macro-scale into consideration must be developed. Figure 1 shows a cross-section of a quasi-isotropic composite laminate and illustrates the heterogeneous architecture of the material. Material heterogeneity on the different scales are described as:

*Micro-scale heterogeneity:* The NCF composite is built of parallel oriented fibre tows in a layer stitched together with neighbouring layer(s) of fibre tows oriented in other direction(s), typically with a polyester thread. Distinct fibre tows in a NCF lamina (or layer) are readily seen in Fig. 1. Heterogeneity on the micro-scale is inherent to the fibre-matrix microstructure within these distinct fibre tows (appearing as bundles). Note that this heterogeneity is similar to that found in UD composite lamina commonly treated theoretically with the rule-of-mixture, etc.

*Meso-scale heterogeneity:* There are two features of heterogeneity dominating on the meso-scale, i.e. at the lamina level. Firstly, the ideally straight (non-crimped) fibre tows exhibit different degree of waviness (see Fig. 1 which shows proof of rather high waviness of the 0° fibre tows, extending in the width direction of the picture). Secondly, distinct fibre bundles separated by resin pockets are present rather than the homogeneously distributed fibres in a conventional UD lamina. Both these features must be treated on the meso-scale, either by unit cell descriptions in FE or by homogenization.

*Macro-scale heterogeneity:* The nature of macro-scale heterogeneity for a NCF composite laminate does not differ from that of a UD composite laminate. The heterogeneity is caused by the difference in fibre orientation between the laminae (layers). This is illustrated in Fig. 1. Consequently, correct homogenization treatment of the micro- and meso-scale heterogeneities will allow use of classical laminate theory for modelling structural performance at this level. Nevertheless, use of an RVE-approach may prove necessary to predict strength of the NCF laminate, since strength will be affected by heterogeneity at the micro- and meso-levels. Two distinct differences to the UD composite must, however, be noted: presence of the stitching thread and nesting of the layers.

Modelling of NCF composites at these three levels is described in this paper. The developed models concern constitutive models as well as failure criteria. In the following sections some of the models developed within FALCOM and their validation are presented. The models are presented divided into two groups: engineering-type and detailed RVE-type models depending on their construction.

## 2 Engineering-type models

The engineering-type models developed in FALCOM comprised both constitutive models and failure criteria. The work in FALCOM also concerned models for notched behaviour, impact resistance and interlaminar toughness prediction. This paper is limited to describing the constitutive models and failure criteria. In general these models consider material heterogeneity on the meso-scale.

### 2.1 Constitutive behaviour of NCF composites

An engineering model to account for stiffness loss in NCF composites caused by material irregularity on the meso-scale was developed by Edgren and Asp [2]. In this work, curved beam models are described and corresponding theoretical stiffness knock-down factors due to out-of-plane waviness of the layers are defined. As mentioned earlier and shown in Fig. 1, the individual tows in the NCF layers are not straight. Instead, they feature a wavy pattern where the tow layer waviness is affected by the position of the layer relative to the mould surface, etc. A mathematical model is developed to calculate the effect of tow layer waviness on the axial stiffness of the lamina. Figure 2 illustrates the approach defining the theoretical stiffness knock-down factor,  $\eta$ , for a wavy layer (i.e. the curved beam) related to that of a straight as,  $\eta = \frac{S_1}{S_0}$ .



Fig. 2 Reduced axial stiffness  $E_{xx}$  due to tow waviness.

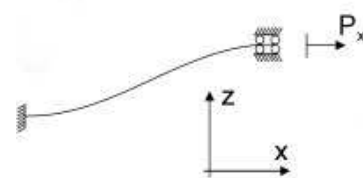


Fig. 3. The curved beam model with fixed fibre tow ends.

The authors [2] were not able to produce closed form expressions for the axial stiffness knock-down factor,  $\eta$ . The models were derived considering a half wavelength of a sinus shaped fibre tow. Figure 3 illustrates the curved beam model with a fixed fibre tow end. Knockdown factors were derived for three different boundary conditions (free, fixed and spring-supported ends). To illustrate the

nature of the knock-down factors influence from wave parameters, i.e. wavelength( $\lambda$ ) and amplitude ( $A$ ), are presented in Fig. 4. In Fig. 4 computed knock-down factors for a lamina using the model, considering a fixed beam end, as a function of amplitude (Fig. 4a) or maximum angle of misorientation (Fig. 4b) are presented ( $A_0 = 78.7 \mu\text{m}$ ). In the figure, predictions for three different crimp wavelengths are plotted. Figure 4 shows that the resulting knock-down factor is dependent on the relationship between crimp wavelength and amplitude, and hence angle of maximum misorientation. The beauty of this method is that the consideration of crimp at the lamina level, only, allows use of conventional classical laminate theory (CLT) on the macro-scale to model laminate behaviour. For this reason the approach provides a method to model NCF composite materials in a similar manner as UD composite at the lamina level.

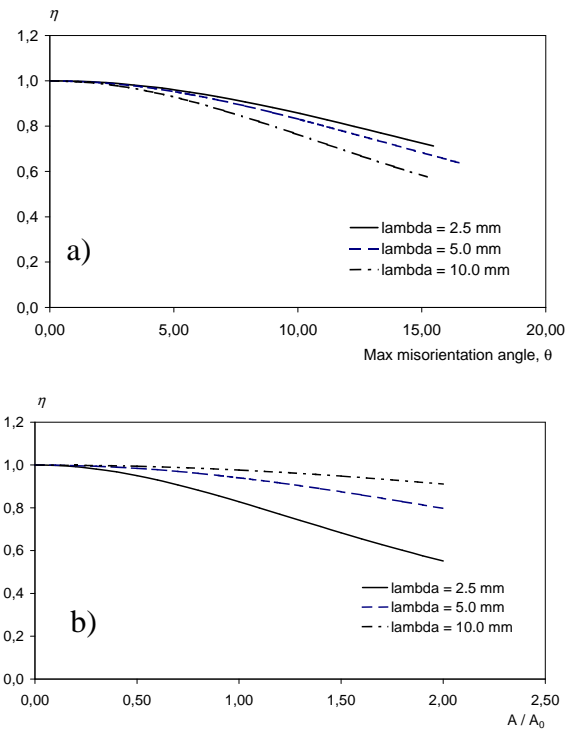


Fig. 4. Sensitivity of the knock-down factor,  $\eta$ , on the: a) wave amplitude and b) maximum angle of misorientation (fixed beam end boundary condition).

### 2.1.1 Validation of the stiffness knock-down model

In order to validate the stiffness knock-down models considering out-of-plane waviness [2] developed in FALCOM were compared to experimental data. Predictions considering measured

fibre tow waviness were compared to test data from the same laminates. Knock-down factors were first derived for each ply in cross-ply and quasi-isotropic laminates considering measured standard deviations of orientation for the individual plies by image analysis. These knock-down factors were then incorporated in the laminate analysis to compute the axial laminate stiffness, reducing the stiffness parallel to the fibres of the individual plies. The original ply properties, considering ideally straight fibre tows in the lamina, were computed homogenizing the material on the micro-scale. Results from predictions employing the knock-down model considering fixed fibre tow ends and experiments are presented in Tables 1 and 2.

Table 1. Axial stiffness and major Poisson's ratio for a NCF cross-ply laminate [2] (standard deviation within brackets).

	Experimental	Predicted ( $\eta < 1$ )
$E_{xx}$ (GPa)	58.1 (1.2)	58.4
$\nu_{xy}$	0.057 (0.017)	0.033

Table 2. Axial stiffness and major Poisson's ratio for a NCF quasi-isotropic laminate [2] (standard deviation within brackets).

	Experimental	Predicted ( $\eta < 1$ )
$E_{xx}$ (GPa)	39.8 (0.91)	40.5
$\nu_{xy}$	0.31 (0.01)	0.33

As illustrated by the results presented in the Tables the model considering fixed fibre tow ends works well to predict the laminate constitutive properties. If one assume straight fibres in the analysis, i.e.  $\eta = 1$ , the predicted axial stiffness for the cross-ply and the quasi-isotropic laminates are 62.7 GPa and 44.1 GPa, respectively, overestimating the laminate stiffness by as much as 10 percent.

## 2.2 General failure criteria for NCF composites

The work at the DLR, Germany, was devoted to development of a generalised failure criterion for NCF composites covering the entire load envelope. For this purpose Juhasz [3] developed a phenomenological, macro-mechanical failure criterion for NCF composites. NCF composites are in many respects very similar to composites made of unidirectional layers. Therefore as basis for this development the so-called "Simple Parabolic Criterion" (SPC) is used which yields very good

results for unidirectional layers and uses Mohr's fracture hypothesis as physical base [4].

NCF composites consist of unidirectional layers with a high in-plane fibre density and additional fibre reinforcements perpendicular to the layers with a much lower fibre density (see Fig. 5). In comparison to composites made of unidirectional layers they therefore possess:

- increased out-of-plane strengths due to additional fibre reinforcements perpendicular to the layers;
- decreased in-plane strengths due to increased in-plane fibre undulation;
- orthotropic material symmetry instead of transversal isotropy.

Due to these differences the SPC developed for unidirectional layers must be adjusted prior to use for NCF composite layers.

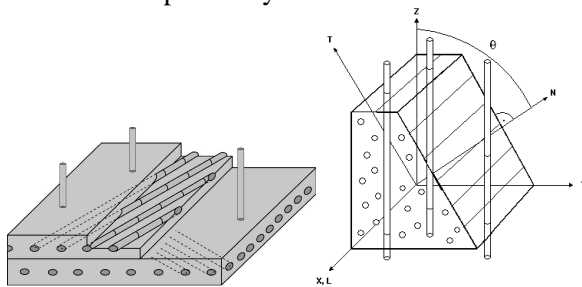


Fig 5. NCF composite fracture planes [3].

The SPC uses a simple max stress criterion for Fibre Fracture (FF):

$$\left| \frac{\sigma_{\parallel}}{R_{\parallel}^{(+,-)}} \right| \quad (1)$$

$\sigma_{\parallel}$  is the stress and  $R_{\parallel}^{(+,-)}$  are the strengths of the layer for tensile (+) and compressive (-) loads in fibre direction. For Inter Fibre Fracture (IFF) the SPC is formulated in stresses and strengths of the fracture plane and is applied to single layers of composites, which are assumed to be homogeneous and defect-free. The stresses of the fracture plane ( $\sigma_N$ ,  $\tau_{NT}$  and  $\tau_{NL}$ ) are obtained by tensor transformation from the stresses with respect to the material axes (see Fig. 5)

The criterion considers strengths of the fracture plane obtained from the strengths of the layer with respect to the material axes. This strength model for unidirectional layers assumes transversal isotropy and has been changed to extend the SPC to NCF

composite layers. The following modification of the SPC is proposed by DLR [3]:

For tensile load normal to the fracture plane,  $\sigma_N \geq 0$

$$\sqrt{(1-p^{(+)})^2 \left( \frac{\sigma_N}{R_N^{(+)}} \right)^2 + \left( \frac{\tau_{NT}}{R_{NT}^{(+)}} \right)^2 + \left( \frac{\tau_{NL}}{R_{NL}^{(+)}} \right)^2} + p^{(+)} \frac{\sigma_N}{R_N^{(+)}} = 1 \quad (2)$$

For compression load normal to the fracture plane,  $\sigma_N < 0$

$$\sqrt{(p^{(-)})^2 \left( \frac{\sigma_N}{R_N^{(-)}} \right)^2 + \left( \frac{\tau_{NT}}{R_{NT}^{(-)}} \right)^2 + \left( \frac{\tau_{NL}}{R_{NL}^{(-)}} \right)^2} + p^{(-)} \frac{\sigma_N}{R_N^{(-)}} = 1 \quad (3)$$

$$R_N^{(+,-)} = \tilde{R}_y^{(+,-)} \sin^2 \theta + \tilde{R}_z^{(+,-)} \cos^2 \theta + \tilde{R}_{yz}^{(+,-)} |\sin 2\theta| \quad (4)$$

$$R_{NT}^{(+,-)} = (\tilde{R}_y^{(+,-)} + \tilde{R}_z^{(+,-)}) |\sin 2\theta| + \tilde{R}_{yz}^{(+,-)} \quad (5)$$

$$R_{NL}^{(+,-)} = \tilde{R}_{xy}^{(+,-)} |\sin \theta| + \tilde{R}_{xz}^{(+,-)} |\cos \theta| \quad (6)$$

The strength parameters  $\tilde{R}$  are obtained by data fitting to experimental results and may differ from the basic strengths of the layer measured in experiments. This is especially true for the shear strengths  $R_{NT}$  and  $R_{NL}$ , which use also different values  $\tilde{R}$  for the tension and compression regime. The new strength model according to Eqs 4-6 provides a continuous interpolation between the strength parameters  $\tilde{R}$  with respect to the material axes.

### 2.2.1 Validation of the modified SPC

Validation of the modified SPC criterion is incomplete. This is due to the fact that independent strength parameters must be measured in separately designed tests. Such tests were never designed nor performed in FALCOM. For this reason, DLR was advised to compute strength properties by back-calculations from tests performed. Furthermore, where test data was not available, an attempt to estimate missing properties by making reasonable assumptions was made. DLR [5] makes the following remark on the difficulty to establish data for a full envelope criterion like the modified SPC: "Since the NCF composites are multidirectional laminates by nature, the transverse properties of UD layers within an NCF composite are not easily assessed, because they are concealed by the high strength and stiffness of the fibres in the neighbouring layers. Consequently it is questionable, if an experimental concept can be developed that is

able to provide the necessary 3D strength data for UD NCF layers". This statement, although focussed on transverse lamina properties has proven to describe a general obstacle when analysing strength of NCF composite laminates. The reason for this is that using general laminate theory strength data for all plies are required. However, these data do depend on the laminate architecture and composite process. This is explained by the effect that lay-up (NCF processing, such as  $\pm 45^\circ$  process vs. a  $0^\circ/90^\circ$  process in the stitch operation, or moving from biaxial to tri- or quadriaxial NCF blankets in the preform) and composite process (e.g. RIFT vs. RFI) have on the fibre tow waviness and fibre tow layer nesting.

Despite the incomplete validation of the modified SPC, and the present uncertainties in how some strength characterisation should indeed be performed for this purpose, the criterion is ruled appropriate for use in analysis of NCF composites. This is motivated by the rigorous physical foundation on which it relies. The criterion has for this reason been implemented in the FALCOM design tool developed by ESI Software.

### 2.3 Compressive failure

Compressive strength of NCF composites has been reported as being as low as half of that in tension [6]. The compressive strength is known to be strongly affected by the material internal structure [7]. The main reason for the low compressive strength is the heterogeneous meso-scale structure, especially fibre tow waviness, of NCF laminates.

The dominating mechanism of compressive failure is plastic fibre microbuckling [8]. This mechanism is a plastic shear instability where initially misaligned fibres cause shear strains to localise in a small region. Fibres fail into small segments, which rotate under increased load. The fibre segments form a band, called kink band, with fibre segments rotated an angle  $(\phi_0 + \phi)$  from the main fibre direction. The kink band grows at an angle  $\beta$  to the fibre direction. A schematic of a kink band in a unidirectional composite is presented in Fig. 6a.

Fleck and Budiansky [10] derived an expression Eq. 7 for the response of a kink band in a rigid-perfectly plastic material to remote loading by axial compressive stress and shear stress, see Fig. 6a.

$$\sigma_x^\infty = \frac{\alpha \tau_y - \tau_{xy}^\infty}{(\phi_0 + \phi)} \quad (7)$$

Where  $\sigma_x^\infty$  is the remote longitudinal stress in the composite,  $\tau_y$  is the composite shear yield strength,  $\tau_{xy}^\infty$  is the remote shear stress in the composite,  $\phi$  is the additional fibre rotation caused by the remote loading and  $\alpha = \sqrt{1 + R^2 \tan^2 \beta}$ ,  $R = \sigma_{Ty} / \tau_y$ , where  $\beta$  is the kink band angle (see Fig. 6a) and  $\sigma_{Ty}$  is the yield stress in pure transverse tension.

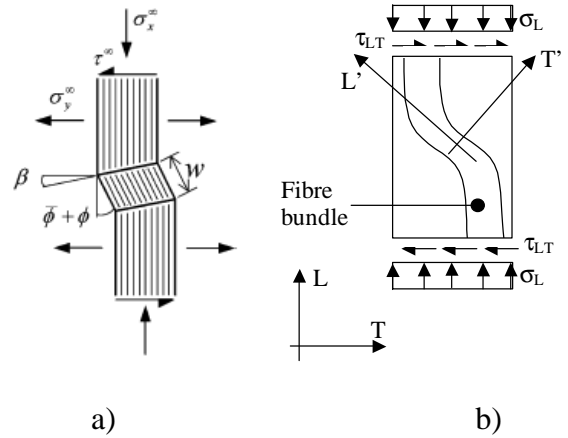


Fig. 6. (a) Kinking of a band with width  $w$ ; (b) Schematic of fibre bundle waviness in NCF, from [9].

In FALCOM Edgren and co-workers [9] suggested a method that allows the criterion by Fleck and Budiansky (Eq. 7) to be used on the homogenized laminas in e.g. CLT. Here the criterion is applied to the composite material within fibre tows. A schematic of a fibre tow in a NCF composite unit is seen in Fig. 6b.

The criterion in Eq. 7 is applied in the  $L'-T'$  system, following the crimped fibre tow. Assuming linear elastic response, Eq. 7 is rearranged to instead be applicable in the lamina coordinate system,  $L-T$ :

$$\frac{\sigma_L}{\sigma_{c0}} + \frac{\tau_{LT}}{\tau_{LT0}} \quad (8)$$

In Eq. 8  $\sigma_L$  and  $\tau_{LT}$  are the stresses acting on the NCF composite lamina.  $\sigma_{c0}$  and  $\tau_{LT0}$  is the uniaxial compressive strength and shear strength of the NCF lamina material respectively. Hence, Eq. 8 allows the strength parameters needed to be determined from tests on the NCF composite, and not its constituents. Nevertheless, since the manufacturing parameters affect the material structure and thus its properties measurements on isolated individual plies may still be difficult.

### 2.3.1 Validation of kink band criterion

As stated above, design parameters (i.e. ply strength and constitutive properties) depend on the NCF composite architecture. That is, ply strength must be measured for the material configuration in which it will be used (that is same NCF process parameters and same composite lay-up). Consequently, e.g. the axial compressive ply strength data for a quasi-isotropic (QI) laminate must be achieved for the QI laminate, made from e.g. bi-axial NCF blankets, and not from UD compression tests as advisable for laminated composites made from pre-preg.

In a first attempt to determine the strength parameters in Eq. 8, tests were performed on the QI laminate, loaded in compression parallel to the 0°-tow plies. Through CLT the longitudinal compressive strength,  $\sigma_{c0}$ , of the ply material was calculated. Here it was assumed that failure of a compression loaded QI specimen is governed by the strength of the most highly loaded ply, in this case the 0°-ply. The pure shear strength,  $\tau_{LTO}$ , was determined using an in-plane shear test in compression. This test was performed on cross-ply laminates, rotated 45° to the direction of loading. Furthermore, compression tests were performed on specimens, which were cut at five different off-axis angles,  $\theta$ , (angle between specimen longitudinal loading direction and 0°-fibre direction);  $\theta = 0^\circ, 5^\circ, 10^\circ, 15^\circ$  and  $20^\circ$ . In these specimens, the 0°-layer becomes the  $\theta$ -layer and remains the highest loaded ply. Results from all these tests are plotted in Fig. 7.

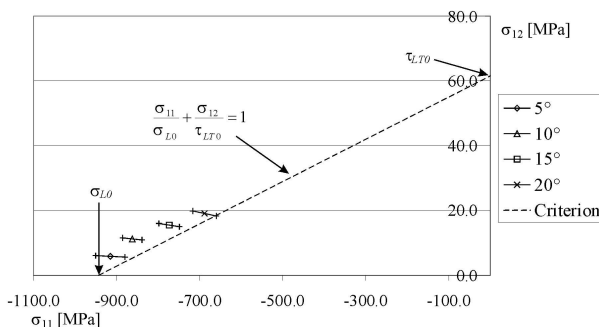


Fig. 7. Stresses in 0°-plies at specimen failure. Stresses calculated with CLT. Failure criterion according to Eq. 8 plotted with dashed line, from [9].

As shown in Fig. 7 the experimental results are in fair agreement with the criterion. The criterion expressed in Eq. 8 requires measurement of two strength parameters: the uniaxial compressive strength and the shear strength of the kinking lamina. However, the criterion is only valid if fibre kinking drives failure. Tested off-axis specimens,

with 0° to 20°-off axis angles, all failed by fibre kinking. However, the specimens subjected to pure shear did not. Obviously, it is hard to think of a pure shear test that would result in fibre kinking. For this reason, no shear strength measured with such a test, e.g. Iosipescu or  $\pm 45^\circ$  tensile or compression tests, will be physically meaningful for validation of the criterion. Consequently, the off-axis compression tests are employed to determine the strength parameters  $\sigma_{c0}$  and  $\tau_{LTO}$ . Figure 8 illustrates the derivation of these parameters following a best-fit procedure of the criterion in Eq. 8.

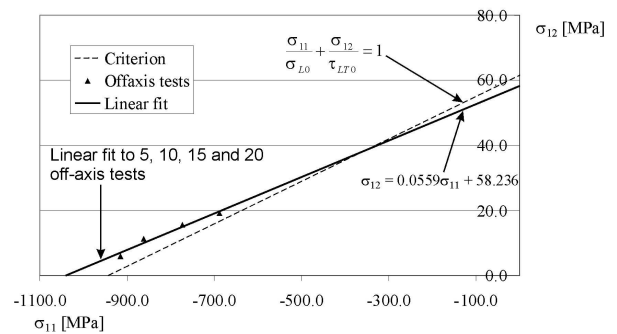


Fig. 8. Linear fit to experimental values compared with prediction from criterion, from [9].

A linear fit through the four experimental points deviates slightly from the dashed line, see Fig. 8. This thus implies that the longitudinal compressive strength,  $\sigma_{L0}$ , is underestimated by an ordinary compression test. This is supported by observations on tubular specimens by Jelf and Fleck [11]. Extrapolation of the linear fit through the off-axis points yields longitudinal compression strength of -1042 MPa. This is approximately 10% higher than the compressive strength retrieved from the 0°-compression test. Likewise, extrapolation to the shear axis yields that the shear strength is slightly overestimated by the in-plane shear test. The extrapolated shear strength is approximately 6% lower than the measured shear strength.

In conclusion, off-axis tests provide a way for measurement of the strength input parameters required to predict compressive strength of NCF composites using Eq. 8. Based on these results, it is recommended that off-axis tests be used for determination of strength parameters in the criterion.

### 3 RVE-type models

Detailed stress analyses of NCF laminates (i.e. on the macro-scale) are recommended by a number of partners in FALCOM [5]. Such analyses employ detailed definitions of RVEs, taking into

account the true meso-structure or homogenizations of the meso-scale features of the NCF. In this section two approaches to detailed FE analysis of NCF composites performance developed within the FALCOM project are presented.

The use of detailed RVE models is considered useful to obtain accurate strength prediction of NCF composites. Furthermore, detailed RVE models may also assist the selection of NCF blanket configuration for a particular application. For instance, it may provide guidance to what stitch fibre tension or fibre tow gap, etc. that should be used for the required performance of a NCF reinforced composite.

### 3.1 Detailed FE analysis scheme

Macro-scale models based on development of RVEs have been put forward by AICIA, among others. The macro-scale model proposed by AICIA is a fully three-dimensional finite element model and is a generalisation of the RUC meso-scale model into an RVE [12]. The RVE is built by stacking several RUC shifted and stitched together, taking into account the specific macro-mechanical parameters such as ply orientation, stacking sequence, etc. An example of the AICIA RVE FE-model is presented in Fig. 9. The dark (purple) regions in the model refer to resin pockets in the gaps between fibre tows. The bright (blue) regions represent fibre tows (the fibres in each tow are oriented along the largest dimension of the tow).

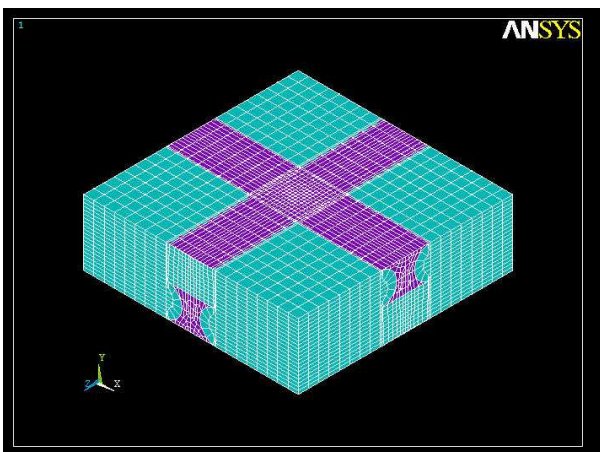


Fig. 9. RVE of a 0°/90° NCF laminate [5].

All the AICIA local models created are based on a basic cell, a quarter of the original RVE due to symmetric properties of the RVE and they are defined through a combination of the physical parameters: crimp angle; gap distance; constituent mechanical properties and stacking sequence. The

parameters gap distance and crimp angle as defined by Paris et al. [12] are presented in Fig. 10.

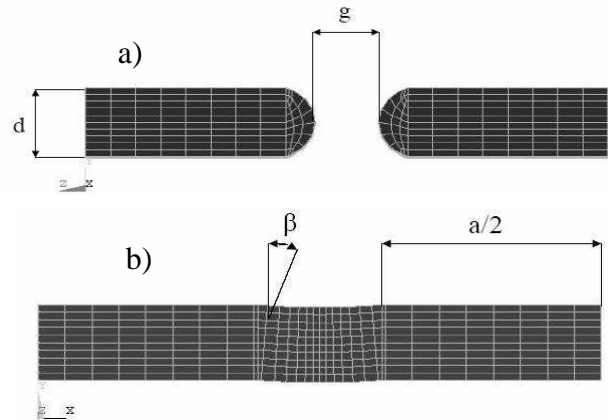


Fig. 10 a) Tows of thickness  $d$  with a gap,  $g$ ; b) Tow with crimp parameters  $\beta$  and  $a$ , from [12].

The material model used for the out of plane shear performance of the tows has followed a non-linear behaviour curve [12]. The reason for the use of this feature is because the raise of high shear stresses, mainly over the more crimped elements, has been directly connected to the failure under compressive loading, and a non-linear shear response of the tows is needed to model the collapse of the laminate under compression loading.

The boundary conditions applied at the faces of the model serve to force the given stress state, obeying displacement compatibility with the rest of the structure.

#### 3.1.1 Validation

In the analysis by AICIA elastic properties of the fibre tows were predicted using conventional rule-of-mixture and Halpin-Tsai approaches. The laminate properties were then computed using a general theory of laminates, imposing a maximum curvature,  $\beta$ , of 3° and a finite element analysis (cross-ply laminates only). Comparison between AICIA predictions and FALCOM test results shows that the predictions usually overestimate the laminate stiffness by 10-20%. Lower stiffness predictions are achieved for the RIFT laminates due to the low stiffness of the resin. This trend is confirmed by the experimental results. Analyses of cross-ply laminates using the FE-approach reveal that crimp angles in the range 9-15° are required to achieve predictions of laminate axial stiffness and Poisson's ratio which are consistent with those measured for the laminates.

The AICIA model has also been assessed for compressive failure prediction. For validation the same test case to that addressed by Drapier and

Wisnom [13] was analysed by the 3D-FE model predictions. The predicted failure mechanism was identical in the two studies. That is, failure is predicted to occur as a result of high shear stresses in the  $0^\circ$  tows, at positions where the crimp angle,  $\beta$ , has its maximum. The high shear stresses are related to both the  $0^\circ$  tow maximum misalignment angle,  $\beta$ , and to  $0^\circ$  tow non-linear shear behaviour. Consequently, the composite fails in compression by a mechanism similar to fibre microbuckling. Drapier and Wisnom [13] refer to this overall instability as  $0^\circ$  tow plastic mesobuckling, and it is shown to control the predicted overall response of the NCF composite, cf. kink band criterion in previous section.

### 3.2 Homogenized RVE models of NCF laminates

In contrast to the RVE-type model considering the distinct composite features (fibre tows, resin pockets and stitch threads etc.) RVE-type models based on homogenized properties were also suggested in FALCOM [14, 15]. The NCF composite may be visualised as the one presented in Fig. 11. The figure illustrates areas consisting of resin only (marked M), fibre bundles oriented  $90^\circ$  to the x-direction, fibre bundles oriented parallel to the x-direction ( $0^\circ$ -direction), and  $0^\circ$ -bundles with an off-set angle extending out-of-plane. Obviously, Fig. 11 presents a simplified view of the actual NCF composite, c.f. Fig. 1. For instance, the elliptic shape of the off-axis bundles is not considered, neither is the true shape of the resin pockets accounted for and nor is the wavy shape of the axial bundles considered. Nevertheless, idealisations like these are admissible for modelling purposes. In addition, the statistical variations of the parameters considered must be accounted for. This is done in the formulation of Representative Volume Elements (RVEs) and Repeatable Unit Cells (RUCs) in FEM.

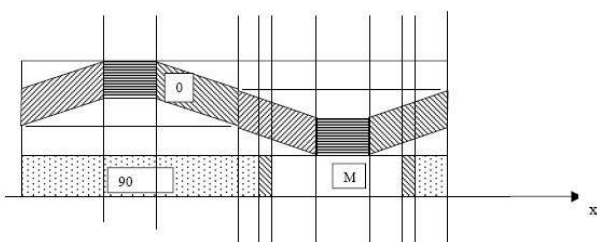


Fig. 11. Imperfect internal structure of the NCF composite in its division in elements by vertical lines, From [5].

Consequently, the NCF composite can be divided in elements as shown in Fig. 11 and each element is an object containing several materials

(sub-elements) and possibly damage, i.e. matrix cracks and delamination. Luleå University of Technology pursued this route and applied an iso-strain assumption for each meso-element. The fibres in Fig. 11 are shown just for illustration, the micro-scale homogenization over bundles is already performed and they are considered as homogeneous anisotropic materials.

#### 3.2.1 Validation homogenization approach

The iso-strain meso-element model was validated by comparison to results from accompanying FE-analyses [14]. It was found that for stiffness calculations the homogenized meso-element RVE model provide sufficient accuracy compared to the 3D-FE model used for reference.

Damage evolution analysis in bundle composites requires detailed information about the transverse strain in the fibre tow, which governs transverse cracking in NCF composites. The iso-strain approach is inadequate for this purpose since in this model the strain in each meso-element is the same. For this reason, Mattson and co-workers [14] extended their homogenization model to consider a super-element. Here it is assumed that the composite consist of “super-elements” for which the stiffness matrix can be obtained by an iso-strain assumption for constituents, thus reducing the inherently 3D stress problem to a 2D problem.

## 4 Concluding remarks

The developed models in FALCOM are truly ample. They range from rigorous analytical expressions for stiffness and strength analysis to detailed FE formulations with complex descriptions of the material meso-structure. The current paper illustrates this variation in approaches taken for modelling the in-plane material mechanical properties. The local models consider detailed or homogenized material descriptions on the micro- and meso-scales. The parameters defined comprise waviness variables, as wavelength and amplitudes, resin regions and gap distances, etc.

Some key findings from the validation of the local models are summarised as:

- Both analytical and numerical models accurately model in-plane stiffness properties;
- In-plane strength predictions for the entire stress envelope has been realised by the development of the modified simple parabolic criterion (SPC);

- Validation of strength properties for individual NCF lamina is problematic. However, such strength parameters must be used if one is to employ conventional laminate analysis schemes. The problem stems from that the waviness properties caused by the NCF architecture and composite process cannot be isolated in a UD NCF model material, and can hence not be directly measured in a test;
- Detailed RVE-type models rely on access to reliable material data for the constituents, i.e. the resin, impregnated fibre tows and stitch thread. Again, such data is not easily measured in tests.

## 5. Acknowledgements

The work by FALCOM colleagues is gratefully acknowledged. The partners were: QinetiQ (Co-ord), NLR, DLR, CIRA, Alenia, AIRBUS-ES, AICIA, EADS-M, AIRBUS-ES, AIRBUS-UK, DEVOLD AMT, Imperial College, ESI Software, ESI GmbH, FACC AG, University of Dresden, Luleå University of Technology, University of Naples, University of Twente and Toho Tenax Fibers.

## 6 References

- [1] FALCOM, "Failure, performance and processing prediction for enhanced design with non-crimp-fabric composites". EU-project, contract No. G4RD-CT-2001-00694.
- [2] Edgren F. and Asp L.E., "Approximate analytical constitutive model for non-crimp fabric composites". *Composites Part A*, Vol 36, pp. 173-181, 2005.
- [3] Juhasz J., "Ein neues physikalisch basiertes versagenskriterium für schwach 3D-verstärkte faserverbundlaminate" (in German), PhD Dissertation, 2003, TU Braunschweig, Germany.
- [4] Cuntze R.G., Deska R., Szelinski B., Jeltsch-Fricker R., Meckbach S., Huybrechts D., Kopp J., Kroll L., Gollwitzer S., and Rackwitz R., "Neue Bruchkriterien und Festigkeitsnachweise für unidirektionalen Faserkunststoffverbund unter mehrachsiger Beanspruchung - Modellbildung und Experimente". *Fortschrittsberichte VDI 5 (506)*, VDI Verlag, Düsseldorf, 1997.
- [5] Asp, L.E., "Competing factors in the selection and design of NCF architectures (process/performance optimisation). Validation of local models by comparison with coupon data". FALCOM Deliverable D4.5-01, FALCOM/WP4/SI/PM004, 2005.
- [6] Asp L.E., Edgren F., and Sjögren A., "Effects of stitch pattern on the mechanical properties of non-crimp fabric composites," *Proceedings of 11<sup>th</sup> European Conference on Composite Materials*, Rhodes, Greece, 2004.
- [7] Edgren F., "Physically based engineering models for NCF composites". PhD Dissertation, 2006, The Royal Institute of Technology (KTH), Sweden.
- [8] Fleck N., "Compressive failure of composite materials". *Advances in Applied Mechanics*, New York, pp. 43-117, 1997.
- [9] Edgren F, Asp L.E. and Joffe R., "Failure of NCF composites subjected to combined compression and shear loading". *Composites Science and Technology*, Vol 66, pp. 2865-2877, 2006.
- [10] Fleck N. and Budiansky B., "Compressive failure of notched carbon fibre composites due to microbuckling". in: Dvorak G.J. (ed.), *Inelastic deformation of composite materials*, Springer, New York, pp. 43-117, 1990.
- [11] Jelf PM, Fleck NA. The failure of composite tubes due to combined compression and torsion. *Journal of Material Science*, Vol. 29, pp. 3080–3084, 1994.
- [12] Paris F., Gonzalez A., Graciani E., Flores M. and del Castillo E., "A 3D FEM study of compressive behaviour of non-crimp fabrics". *Proceedings of 11<sup>th</sup> European Conference on Composite Materials*, Rhodes, Greece, 2004.
- [13] Drapier S. and Wisnom R.M., "Finite-element investigation of the compressive strength of non-crimp-fabric-based composites". *Composites Science and Technology*, Vol. 59, pp. 1287-1297, 1999.
- [14] Mattsson, D., "Mechanical performance of NCF composites", PhD Dissertation, Luleå University of Technology, Sweden, 2005.
- [15] Mattsson D., Joffe, R., and Varna, J., "Methodology for characterization of internal structure parameters governing performance in NCF composites". *Composites: Part B*, Vol. 38, pp. 44-57, 2007.

